Progress in Oceanography 142 (2016) 58–71

Contents lists available at ScienceDirect

Progress in Oceanography

journal homepage: www.elsevier.com/locate/pocean

The influence of oceanographic features on the foraging behavior of the olive ridley sea turtle *Lepidochelys olivacea* along the Guiana coast

Philippine Chambault [a,*], Benoît de Thoisy [b], Karine Heerah [c], Anna Conchon [d], Sébastien Barrioz [b], Virginie Dos Reis [b], Rachel Berzins [e], Laurent Kelle [f], Baptiste Picard [g], Fabien Roquet [h], Yvon Le Maho [a], Damien Chevallier [a]

[a] DEPE-IPHC, UMR 7178, CNRS-UdS, 23 rue Becquerel, F-67087 Strasbourg cedex 2, France
[b] Association Kwata, 16 avenue Pasteur, BP 672, F-97335 Cayenne cedex, France
[c] LOCEAN-UMR 7159, 4 place Jussieu, 75252 Paris cedex 05, France
[d] Collecte Localisation Satellites, Direction Océanographie Spatiale, 8-10 rue Hermès, 31520 Ramonville, France
[e] Office National de la Chasse et de la Faune Sauvage – Cellule technique Guyane, Campus agronomique, BP 316, 97379 Kourou cedex, France
[f] WWF Guyane, N°5 Lotissement Katoury, F-97300 Cayenne, France
[g] Centre d'Études Biologiques de Chizé, UMR 7372 CNRS – Université de La Rochelle, 79360 Villiers-en-Bois, France
[h] Stockholm University, Department of Meteorology (MISU), Sweden

ARTICLE INFO

Article history:
Received 13 August 2015
Received in revised form 28 January 2016
Accepted 28 January 2016
Available online 4 February 2016

ABSTRACT

The circulation in the Western Equatorial Atlantic is characterized by a highly dynamic mesoscale activity that shapes the Guiana continental shelf. Olive ridley sea turtles (*Lepidochelys olivacea*) nesting in French Guiana cross this turbulent environment during their post-nesting migration. We studied how oceanographic and biological conditions drove the foraging behavior of 18 adult females, using satellite telemetry, remote sensing data (sea surface temperature, sea surface height, current velocity and euphotic depth), simulations of micronekton biomass (pelagic organisms) and *in situ* records (water temperature and salinity). The occurrence of foraging events throughout migration was located using Residence Time analysis, while an innovative proxy of the hunting time within a dive was used to identify and quantify foraging events during dives. Olive ridleys migrated northwestwards using the Guiana current and remained on the continental shelf at the edge of eddies formed by the North Brazil retroflection, an area characterized by low turbulence and high micronekton biomass. They performed mainly pelagic dives, hunting for an average 77% of their time. Hunting time within a dive increased with shallower euphotic depth and with lower water temperatures, and mean hunting depth increased with deeper thermocline. This is the first study to quantify foraging activity within dives in olive ridleys, and reveals the crucial role played by the thermocline on the foraging behavior of this carnivorous species. This study also provides novel and detailed data describing how turtles actively use oceanographic structures during post-nesting migration.

1. Introduction

The circulation in the Western Equatorial Atlantic is characterized by a highly dynamic mesoscale activity driven by the North Brazil Current (NBC) and the North Equatorial Countercurrent (NECC) (Pauluhn and Chao, 1999; Froidefond et al., 2002; Fratantoni and Richardson, 2006) – see Appendix A. The NBC originates from the South Equatorial Current, and carries upper-ocean waters northwards to the equator. During the boreal fall season, a large part of the NBC at approximately 7°N–48°W retroflects eastwards, feeding the NECC (Lumpkin and Garzoli, 2005). This retroflection generates anticyclonic eddies with radii up to 200 km, which then move toward the Caribbean for several months every year (Didden and Schott, 1993).

These mesoscale features transport and disperse nutrient-rich waters originating from the Amazon River, further east (Baklouti et al., 2007). The Amazon is the largest river in the world, and discharges large amounts of sediment as well as particulates and chromophoric dissolved organic materials ($115 \cdot 10^7$ tons per year) into the Equatorial Atlantic Ocean (DeMaster et al., 1996; Meade, 1996). In this context, the Amazon plume strongly influences the oceanographic and biochemical conditions in the north-eastern part of the South American continental shelf, stretching from the

* Corresponding author.
E-mail address: philippine.chambault@gmail.com (P. Chambault).

http://dx.doi.org/10.1016/j.pocean.2016.01.006
0079-6611/

North Brazilian coast to the Caribbean, making it a highly productive area (Muller-Karger et al., 1988; DeMaster et al., 1996).

The French Guiana continental shelf reaches from the Amazon River to the Trinidad Island sector and hosts three sea turtles species, namely the green turtle *Chelonia mydas* (Baudouin et al., 2015; Chambault et al., 2015), the leatherback *Dermochelys coriacea* (Fossette et al., 2006, 2010a,b) and the olive ridley *Lepidochelys olivacea* (Kelle et al., 2009; Plot et al., 2015). Although all three species remain on the continental shelf throughout the breeding and nesting seasons (Fossette et al., 2006; Georges et al., 2007), they exhibit different dispersal strategies during their post-nesting migration (Fossette et al., 2010b; Chambault et al., 2015; Plot et al., 2015; Baudouin et al., 2015). Only the olive riley sea turtles remain on the French Guiana continental shelf after the nesting season (Plot et al., 2015).

The olive ridley population that nests in French Guiana remains within the neritic domain during its northwestward post-nesting migration, which is an unusual habitat, confirming that this species can occupy different habitats according to the population (Polovina et al., 2004). Olive ridleys also exhibit behavioral plasticity in terms of dispersal and diving behavior through the use of different habitats according to the individual, i.e. the continental shelf, the continental slope or deep waters (Plot et al., 2015). This post-nesting migration, over the Guiana basin, occurs in the equatorial waters of the Atlantic, making this site unique as it is on the very periphery of the species range (Grinnell, 1917). Furthermore, nothing is known to date about how this population uses mesoscale features to forage at its range boundaries.

This study is the first to investigate the role of mesoscale features in the foraging behavior of olive ridley sea turtles. Mesoscale features such as eddies, fronts and upwelling/downwelling are highly variable in size and duration, covering from 100 km to 500 km and lasting anywhere between 10 and 100 days (Croxall, 1987). They are expected to strongly influence the foraging strategies of pelagic organisms, especially marine megafauna (Bailleul et al., 2010). Indeed, these oceanic structures contribute to ocean mixing, enhancing primary productivity at low trophic levels and concentrating prey for megafauna organisms, thereby affecting the entire food chain through bottom-up processes (Lévy, 2008). Recent studies in two different populations of elephant seals have demonstrated links between foraging behavior and eddies – fronts (Campagna et al., 2006; Bailleul et al., 2010; Dragon et al., 2010). Similar results have been obtained in cetaceans (Davis et al., 2002), seabirds (Weimerskirch et al., 2004; Pinaud and Weimerskirch, 2005; Cotté et al., 2007; Tew-Kai and Marsac, 2009) and sea turtles (Polovina et al., 2006; Lambardi et al., 2008), indicating that areas of high productivity provide feeding grounds for a broad range of marine megafauna species.

To date, the identification of eddies and fronts has mainly been based on remote sensing data such as Sea Surface Temperature (SST), Sea Surface Height (SSH), primary production and oceanic circulation (current velocity). However, an innovative modeling approach based on the distribution of pelagic preys has emerged over the last decade: the Spatial Ecosystem And Population Dynamics Model (SEAPODYM) (Lehodey et al., 2008). This model of mid-trophic organisms is based on several types of prey that are vertically distributed within the water column, i.e. the micronekton. The technique has been initially used to predict tuna population dynamics (Lehodey et al., 2010a,b; Lehodey et al., 2012; Sibert et al., 2012) and recently cetacean distribution (Lambert et al., 2014), and also to simulate turtle movements (Abecassis et al., 2013).

Several techniques have been developed to detect foraging events. In the horizontal dimension, the identification of Areas of Restricted Search (ARS) was based on the detection of decrease in travel speed and increase in turning angles (Kareiva and Odell, 1987; Robinson et al., 2007; Dragon et al., 2012). The detection of ARS has helped to identify foraging activity in numerous species via a wide range of techniques (Fauchald and Tveraa, 2003; Weimerskirch et al., 2004; Jonsen et al., 2005, 2006, 2007; Gaspar et al., 2006; Pinaud, 2008; Bailey et al., 2008; Barraquand and Benhamou, 2008; Dragon et al., 2012; Plot et al., 2015). There is a significant depth structure to foraging behavior within the water column in particular areas of prey aggregation (Fuiman et al., 2002; Watanabe et al., 2003; Mitani et al., 2003), making it essential to take the vertical dimension into account as well (Bailleul et al., 2008). New techniques using acceleration data from data loggers placed on pinnipeds (Viviant et al., 2014; Labrousse et al., 2015) and sea turtles (Okuyama et al., 2009; Fossette et al., 2010a,b, 2012a,b) have made it possible to identify prey capture attempts during the dives. However, such techniques were mostly inapplicable to low resolution datasets, which require tag retrieval after tracking (Heerah et al., 2014, 2015). Consequently, vertical foraging activity is often identified and quantified using foraging indices such as bottom time, dive shape (Fedak et al., 2001; Dragon et al., 2012) or, more recently, hunting time (Heerah et al., 2015). This study applies the hunting time index to olive ridley sea turtles for the first time, making it possible to estimate the time spent foraging within-dives.

In 2013 and 2014, satellite tags were deployed on 20 adult female olive ridley sea turtles to assess the influence of oceanographic and biological features on their foraging behavior in horizontal and vertical dimensions during their post-nesting migration from French Guiana. This study aims to (1) analyze horizontal movements in relation to remote sensing data and micronekton biomass, then to (2) quantify and link foraging events within dives to *in situ* data directly recorded within the water column.

2. Materials and methods

2.1. Ethics statements

This study met the legal requirements of the country in which the work was carried out, and followed all institutional guidelines. The protocol was approved by the "Conseil National de la Protection de la Nature" (CNPN, http://www.conservation-nature.fr/acteurs2.php?id=11), which is under the authority of the French Ministry for ecology, sustainable development and energy (permit number: 09/618), and acts as the ethics committee for French Guiana. The fieldwork was carried out in strict accordance with the recommendations of the Police Prefecture of Cayenne, French Guiana, France, in order to minimize any disturbance of the animals.

2.2. Study area and tag deployment

During the 2013 and 2014 nesting seasons, 20 adult female olive ridleys were equipped with satellite tags on the beaches of Remire-Montjoly (4.53°N–52.16°W, Cayenne, French Guiana). Eight Argos-linked Fastloc GPS tags (MK10, Wildlife Computers Redmond, WA, USA) were deployed from July to August 2013. Twelve Conductivity Temperature Depth Fluorometer-Satellite Relayed Data Loggers (CTD-SRDL, Sea Mammal Research Unit, University of St. Andrews, Scotland) were fitted during the same period in 2013 ($n = 2$) and 2014 ($n = 10$).

Using a red light to minimize disturbance, the satellite tags were attached during night-time egg laying, i.e. at the only moment when individuals are static – for details see Baudouin et al., 2015. The carapace was cleaned with scrapers, water and acetone, then the tags were fixed to the carapace as close as possible to the head using an epoxy resin, with the antenna facing

forward. To allow the resin to dry completely, turtles were then herded into a pen for approximately 2 h before being released. During tag deployment, measurements of the Curved Carapace Length (CCL) were also taken.

2.3. Data collected from the tags

The procedure for data extraction of the migratory routes is described in Baudouin et al. (2015). Diving behavior data recorded by the tags describe specific diving parameters, namely maximum dive depths and dive durations and *in situ* temperature data, binned as 4-h period histograms. Maximum depths were collected in different bins, every 10 m from 10 to 100 m, then every 50 m from 100 to 250 m. Similarly, maximum dive durations were stored from 30 s to 1 min, then every minute from 1 to 5 min, and finally every 10 min from 10 to 60 min. *In situ* temperatures from 20 to 32 °C were recorded during dives with a resolution of one degree Celsius. Tags also supplied Time At Depth (TAD) and Time At Temperature (TAT), defined as the proportion of time (in %) spent at each depth and the temperature range, respectively.

The 12 CTD-SRDL tags provided the locations of turtles via the Argos Doppler Location algorithm (Lopez et al., 2014), data on diving behavior including dive depth, dive duration, time at depth and duration of post-dive surface intervals, and oceanographic data in the form of vertical temperature and salinity profiles taken during the ascent phase of turtle dives (Boehme et al., 2009). The CTD-SRDL tags were programmed to send summarized dive profiles using the compression algorithm described by Fedak et al. (2001) with four depth records for each dive (instead of 1 maximum depth per dive for the Argos-Fastloc GPS tags). Temperature and salinity data were quality controlled using the procedure described in Roquet et al. (2011), with an estimated accuracy of 0.02 °C in temperature and 0.05 in salinity. Similar CTD-SRDL tags have been extensively used on seals in polar regions over the last decade, and particularly in the Southern Ocean, where they have become a major source of oceanographic data (Roquet et al., 2013). To our knowledge, our study is the first to use CTD-SRDL tags to study sea turtles in a tropical region.

2.4. Data pre-filtering

As the tags were deployed during the nesting season, they recorded both the nesting and migration phases. We therefore performed a spatial query via ArcGIS version 10.1 to identify the date of migration departure based on the distance traveled from the nesting site and the last nesting event (identified thanks to the wet/dry sensor of the tag) to exclude the nesting period from our data, thus ensuring that the migration phase alone was retained in the analysis (Baudouin et al., 2015). A Kalman filtering algorithm was then applied to the locations (CLS, Collecte Localisation Satellites, Toulouse, France) to enhance tag position estimates (Argos and GPS) (Silva et al., 2014). The General Bathymetric Chart of the Oceans (GEBCO) database (http://www.gebco.net/, resolution 30 arc-sec, ~1 km grid) was used to discard any locations on land. The Argos Kalman-filtered locations associated with a swimming speed of over 10 km h^{-1} were also discarded, as well as any locations classed as Z, considered insufficiently accurate.

2.5. Identification of foraging grounds in the horizontal dimension

ARS were identified by applying a two-step procedure to the location data (Argos and GPS of both tag instruments), namely (1) First Passage Time (FPT) analysis (Fauchald and Tveraa, 2003) followed by (2) Residence Time (RT) analysis (Barraquand and Benhamou, 2008). FPT is defined as the time required by an organism to cross a circle of a given radius. The optimal ARS circle radius for each turtle was estimated using the *fpt* function from the *adehabitatLT* package from the R software version 3.1.2 (R Core Team, 2014). Tested radii ranged from 1 to 400 km to ensure the coverage of large foraging movements (Fauchald and Tveraa, 2006). For each track, the relative variance of FPT (log transformed) was plotted against radii to identify the different scales of the searching activity (ARS radius) revealed by a peak of variance at a specific radius. After identifying the optimal ARS scale for each individual, RT analysis was performed on the data to distinguish between the 'transiting' mode (low RT) and the 'foraging' mode (high RT) in both time and space. This was achieved through the temporal detection of ARS periods using Lavielle's segmentation method (2005) from the *adehabitatLT* package (Calenge, 2006).

2.6. Relating horizontal foraging activity to surface biological variables

We related the foraging activity of olive ridleys to the distribution of their prey using the SEAPODYM model, (Lehodey et al., 2010a). SEAPODYM predicts the spatio-temporal distribution of micronekton, the smallest pelagic organisms able to swim against sea currents (individuals measuring from 2 to 25 cm). This model creates an idealized 3-layer ocean simulation, and organisms are classified into six functional groups according to their diel vertical migration behavior (Lehodey et al., 2010a,b).

SEAPODYM takes the carnivorous diet of olive ridleys into account, and encompasses different potential preys including cephalopods, jellyfishes, crustaceans and fishes (Brodeur et al., 2005). The SEAPODYM simulation takes oceanographic components such as currents, temperature, primary production and euphotic depth into consideration and provides micronekton biomass and production on a regular grid of 0.25° at a weekly resolution. As olive ridleys remain mainly above depths of 80 m, we only considered the first SEAPODYM layer. Groups were split into night and day distributions, e.g. MNKnight and MNKday.

2.7. Relating horizontal foraging activity to surface oceanographic variables

We calculated the total distance traveled and the tracking duration using the *trackDistance* function from the *trip* package (Luque, 2007), then derived the travel speed from this data. To investigate the role of oceanic circulation on turtle movements, surface current data (meridional and zonal components) were extracted daily from the Operational Mercator Global Ocean analysis and forecast system, at a resolution of 0.08° (~9 km) (data available on: http://www.myocean.eu/). Oceanic current velocity and direction were then derived from meridional and zonal components (scalars u and v, respectively). Turtle swimming speed was then calculated with a correction for current velocity to give a proxy of swimming effort (Gaspar et al., 2006; Cotté et al., 2007).

To describe the habitat of olive ridleys at their foraging grounds, we used the daily data of two additional oceanographic variables extracted from the Mercator Ocean model at a spatial resolution of 0.08°: SSH, as an indication of mesoscale activity (Stammer and Wunsch, 1999) and SST, influencing the metabolism of turtles and prey distribution. Sea Surface Salinity was not included because the strong influence of the Amazon River can lead to a bias in the estimation of variables in this region and because other river outputs along the Guiana basin are not taken into account by Mercator.

All the values of these three dynamic variables were then extracted at the locations of each turtle using the *extract.data* function from *SDMTools* package (VanDerWal et al., 2014). Bathymetry, a static covariate, was also extracted from GEBCO at each location.

2.8. Identification of foraging activity in the vertical dimension

We discriminated between benthic and pelagic dives by calculating the difference between the bathymetry at the dive location and the maximum dive depth recorded by the CTD-SRDL for the same location for each dive. Therefore, dives with a maximum depth within 3 m of seabed were classified as benthic dives, and those with a maximum depth beyond 3 m from seabed were pelagic dives. The Argos-linked Fastloc GPS tags ($n = 8$) were not incorporated due to the coarser resolution (1 dive depth every 10 m). At some locations, this depth difference was greater than the bathymetry depth, possibly due to the error generated by the shift between the bad Argos positions and the considerable displacements of the turtle during the dive, caused by variable seabed bathymetry. To get an indication of the shape of the dives, we calculated the Time of Allocation at Depth (TAD) index by using the four inflection points of the summarized profiles provided by the CTD-SRDL tags. Based on Fedak et al.'s method (2001), the TAD was calculated in order to give relevant information about where turtles center their activity within the dives, i.e. V-shaped dives for $0.5 \leqslant \mathrm{TAD} < 0.75$ (exploratory dives) and U-shaped dives for $0.75 \leqslant \mathrm{TAD} < 1$ (foraging activity centered at the bottom of the dive). Following the method of Plot et al. (2015), the average rate of change of depth was fixed at 1.4 m s^{-1}.

After identifying the foraging events in the horizontal dimension, we aimed to quantify the vertical foraging activity within a dive. Prey acquisition in marine megafauna is often assumed to occur during the bottom phase of dives (Houston and Carbone, 1992). However, depending on the species and the structure of the oceanographic environment (which ultimately affects prey distribution in the water column), foraging activity can also occur outside the bottom phase, revealing generalist feeding and opportunistic behavior (Heerah et al., 2014). To estimate the foraging activity within a dive, we used a method that was previously applied for Weddel and elephant seals (Heerah et al., 2014, 2015), and which calculates a foraging index, i.e. the hunting time. This method relies on the detection of the vertical ARS, indicated by an increase in vertical sinuosity and a decrease in vertical speed (Heerah et al., 2014). The authors demonstrated that "hunting" phases, i.e. vertical ARS phases, were associated with more prey capture attempts in both high and low resolution dives (Heerah et al., 2014, 2015). Since vertical sinuosity cannot be calculated for low resolution data (only four dive records per dive), Heerah et al. (2015) determined a low-resolution foraging index (hunting$_{\mathrm{lowres}}$ time) based on the detection of reduced vertical speed, i.e. the rate of change between depth segments within a CTD-SRDL dive. Dive segments associated with a vertical speed below a defined threshold (Heerah et al., 2015) are classified as "hunting" whereas segments associated with a greater vertical speed are considered as "transit". The time spent in hunting segments is then added together for each dive to calculate the total hunting$_{\mathrm{lowres}}$ time.

We adapted this approach to olive ridley low resolution datasets by using the density of the vertical speed to test for several hunting time thresholds, and consequently discriminate between transiting vs. foraging modes. Hunting time was calculated for different thresholds of vertical velocity: from 0.01 to 0.5 m s^{-1}, every 0.1 m s^{-1}. For a series of random dives, a visual exploration of the identified hunting vs. transiting mode was performed to identify the correct threshold. A threshold of 0.04 m s^{-1} appeared as the optimal value to discriminate between the two modes. Once the total hunting time had been calculated for each dive, the associated mean depth was extracted, and the hunting time frequency (in %) was derived from the duration of each dive.

2.9. Relating vertical foraging activity to oceanographic variables of the water column

We used the CTD datasets collected from the tags to associate a temperature and salinity value to each mean hunting depth. However, diving and CTD data were stored in separate datasets that rarely matched in time and space, so we searched for the closest CTD profile in time and space for each dive (time window <48 h and space constraint <30 km, i.e. mean daily distance traveled and lowest resolution of the environmental variables extracted). We also identified the thermocline depth (effect on primary production and distribution of prey) by calculating the temperature gradient for each CTD profile. Some temperature profiles were recorded at very shallow depths with some high temperature gradients in the upper layers, leading to a false identification of the thermocline depth. We also carried out a visual inspection of the temperature profiles of each tag to estimate the approximate thermocline depth, and removed the outliers located above this limit (a depth of up to 20 m). Euphotic depth (hereafter Zeu) was extracted to a grid of $0.25° \times 0.25°$ with a weekly resolution (used in SEAPODYM, provided by CLS, Toulouse) to investigate variations in the vertical accessibility of olive ridley prey (Lambert et al., 2014) and give a proxy of the water turbidity.

We performed a series of Linear Mixed Models (LMM) to relate the hunting time to water mass characteristics, using the R package *nlme* (Pinheiro et al., 2015) and following the steps described in Zuur et al. (2009). Collinear predictors were excluded (Spearman coefficients >0.7 and <−0.7), and the remaining covariates were included as fixed effects, i.e. the temperature at mean hunting depth (hereafter Hunting Temp), thermocline depth and euphotic depth. Salinity data were not incorporated in the LMM due to the low number of profiles recorded. All numeric variables were standardized, i.e. centered and scaled, allowing us to compare the magnitude of the effect for each predictor covariate (Péron et al., 2010). Turtle ID and the year of tag deployment were used as random effects. An autocorrelation term was also added to the models to account for temporal and spatial correlation between dives (Zuur et al., 2009). Similarly, a series of LMM was also fitted to assess the link between the mean hunting depth and oceanographic structures. All the combinations were tried without interactions, then the remaining covariates were incorporated and the models were compared using ANOVA before finally selecting the model with the lowest AIC (Burnham et al., 2011).

2.10. Statistical analysis

All statistical analyses were performed using R software version 3.2.1 (R Core Team, 2014). All samples submitted to statistical tests were first checked for normality and homogeneity of variances by means of the Shapiro–Wilk test. Parametric or nonparametric tests were then used, according to the results. Globally, Mann–Whitney *U* tests were used to compare the environmental variables among the two modes, i.e. transiting vs. foraging, using a significance level of $\alpha = 0.05$. Kruskal–Wallis tests were performed to account for differences between individuals. Values are means ± SD.

3. Results

3.1. Foraging behavior in the horizontal dimension

3.1.1. Trajectories and foraging grounds

The 20 olive ridley sea turtles fitted with either Argos-linked Fastloc GPS tags or CTD-SRDL measured 71.5 ± 2.5 cm CCL (range: 69–75 cm). The tag instruments transmitted on average 438 ± 330 locations, for a tracking duration ranging from 7 days (#130770)

up to 229 days (#130765, Table 1). Two of the 10 turtles equipped during the inter-nesting season in 2014 did not transmit any data, namely individuals #136776 and #136777. In both years, the 18 remaining turtles headed northwestward and remained on the continental shelf off the shores of Suriname and French Guiana, mainly between 20 m and 100 m isobaths (Fig. 1). Only one turtle equipped in 2013 (#130771) reached the Venezuelan coast, traveling over 2776 km. The total distance traveled varied from 412 km (#130770) to 3651 km (#130765, mean: 1502 ± 689 km), whereas the forward linear path to reach foraging grounds was on average 366.8 ± 294.5 km, varying from 41.6 km to 1369 km (#130769 vs. #130771). The average observed speed was 0.45 ± 0.15 m s^{-1} (range: 0.25 ± 0.27–0.78 ± 0.61 m s^{-1}, #131355 vs. #130770, respectively). The real swimming speed corrected for oceanic currents ranged from 0.53 ± 0.32 to 1.10 ± 0.59 m s^{-1} (#131354 vs. #130769, respectively), with an average of 0.69 ± 0.17 m s^{-1}. Average elapsed time to reach the foraging grounds was 30 ± 17 d (range: 1–52 d, #130769 vs. #131355, respectively). The average ARS scale was 34.7 ± 25.6 km radius, ranging from 13 km to 100 km (#130765a and #130766 vs. #130765, respectively).

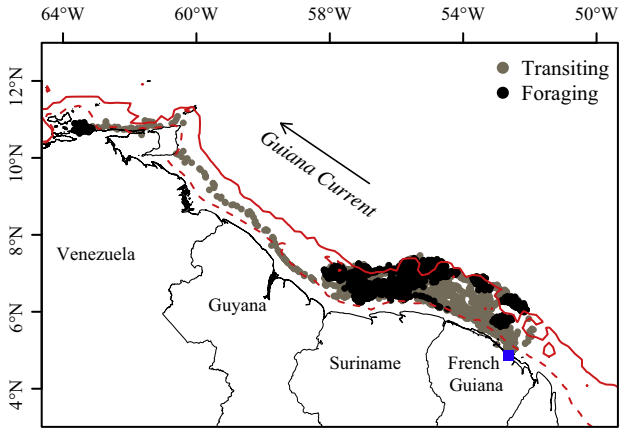

Fig. 1. Locations of the 18 olive ridley turtles equipped in 2013 (n = 10) and 2014 (n = 8) for the two behavioral modes, i.e. transiting (gray) and foraging (black). The blue square indicates the migration departure point, the dotted red line shows the 20 m isobaths and the solid red line indicates the 100 m isobaths.

3.1.2. Habitat use across the Guiana basin

On the Guiana basin scale, olive ridleys remained on the continental shelf during all the tracking duration, presumably avoiding the large eddies that are associated with higher SSH and maximum current velocities reaching up to 1.5 m s^{-1} (Fig. 2). The prevailing current were mainly northwestward, flowing at 0.53 ± 0.22 m s^{-1} at turtle's locations, and the individuals were associated with low SSH, on average 2.9 ± 3.8 cm. For both years of tag deployment, the micronekton biomass was aggregated at the edges of eddies (Fig. 3), supplying the continental shelf in micronekton biomass (mean: 1.7 ± 0.95 g WW m^{-2}). The foraging grounds of olive ridley sea turtles were therefore associated with higher micronekton biomass.

3.1.3. Habitat use at the tracking scale

During their post-nesting migration, olive ridleys remained in quite homogeneous habitats in terms of environmental conditions. Current velocity was slightly but significantly lower when turtles were foraging than when they were transiting (0.50 ± 0.20 vs. 0.58 ± 0.24 m s^{-1}, respectively, Mann–Whitney U test, n = 7885, p < 0.001, Fig. 2). The same pattern was observed for SST, with a very slight difference (28.25 ± 0.67 vs. 28.32 ± 0.65 °C, respectively, Mann–Whitney U test, n = 7885, p < 0.001). The turtles were associated with higher SSH at their foraging grounds (3.12 ± 3.86 vs. 2.48 ± 3.68 cm, respectively, Mann–Whitney U test, n = 7885, p < 0.001, Fig. 2) and deeper bathymetry than while transiting (81.9 ± 77.5 vs. 61.3 ± 63.0 m, respectively, Mann–Whitney U test, n = 7885, p < 0.001). Micronekton biomass during daytime and night were highly correlated, only micronekton during the day was retained for the analysis (Spearman correlation test: R^2 = 0.99, p < 0.001). The micronekton biomass during daytime was relatively high throughout migration for all individuals, and there was no significant difference in micronekton biomass during daytime between the two behavioral modes (1.76 ± 0.92 vs. 1.72 ± 0.97 g WW m^{-2}, respectively, Mann–Whitney U test, n = 7885, p < 0.05, Fig. 3).

3.2. Foraging behavior in the vertical dimension

3.2.1. Diving behavior from Argos-linked Fastloc GPS tags

The 8 Argos-linked Fastloc GPS tags deployed in 2013 provided 4055 records of maximum dive depth and 4583 records of dive

Table 1
Summary of the horizontal movements of the 18 olive ridleys tracked. Values are Mean + SD. PTT indicates individual turtle ID, Nloc the number of locations.

PTT	Start date	End date	Instrument	Nloc	Tracking duration (d)	Distance traveled (km)	Observed speed (m s^{-1})	Swimming speed (m s^{-1})
130764a	23/07/2013	29/09/2013	MK10	586	68	2384	0.58 ± 0.53	0.92 ± 0.52
130765a	20/08/2013	23/10/2013	MK10	457	64	2095	0.60 ± 0.56	1.10 ± 0.56
130766	07/08/2013	10/09/2013	MK10	193	34	1109	0.51 ± 0.50	0.72 ± 0.46
130767	22/07/2013	30/08/2013	MK10	174	39	1226	0.52 ± 0.49	0.72 ± 0.52
130768	04/08/2013	14/10/2013	MK10	262	71	2002	0.56 ± 0.56	0.66 ± 0.58
130769	21/07/2013	08/09/2013	MK10	288	49	1284	0.52 ± 0.58	1.10 ± 0.59
130770	05/08/2013	12/08/2013	MK10	36	7	412	0.78 ± 0.61	0.69 ± 0.54
130771	09/08/2013	05/10/2013	MK10	454	57	2776	0.76 ± 0.57	0.74 ± 0.59
131354	02/08/2013	20/11/2013	CTD-SRDL	1157	110	2174	0.31 ± 0.33	0.53 ± 0.32
131355	02/08/2013	28/12/2013	CTD-SRDL	1314	148	2237	0.25 ± 0.27	0.56 ± 0.30
130764	25/07/2014	15/10/2014	CTD-SRDL	235	82	1218	0.42 ± 0.48	0.60 ± 0.45
130765	02/08/2014	19/03/2015	CTD-SRDL	624	229	3651	0.31 ± 0.34	0.59 ± 0.32
136772	04/09/2014	29/10/2014	CTD-SRDL	223	55	795	0.30 ± 0.32	0.67 ± 0.34
136773	22/09/2014	12/12/2014	CTD-SRDL	285	81	1793	0.40 ± 0.43	0.55 ± 0.40
136774	28/08/2014	13/11/2014	CTD-SRDL	336	77	1632	0.37 ± 0.39	0.54 ± 0.34
136775	10/08/2014	10/10/2014	CTD-SRDL	268	61	1357	0.32 ± 0.37	0.59 ± 0.33
136778	03/08/2014	13/11/2014	CTD-SRDL	425	102	2075	0.35 ± 0.40	0.59 ± 0.38
136779	30/08/2014	28/12/2014	CTD-SRDL	568	120	2608	0.40 ± 0.43	0.59 ± 0.41
				438 ± 330	80.7 ± 49.6	1502 ± 689	0.45 ± 0.15	0.69 ± 0.17

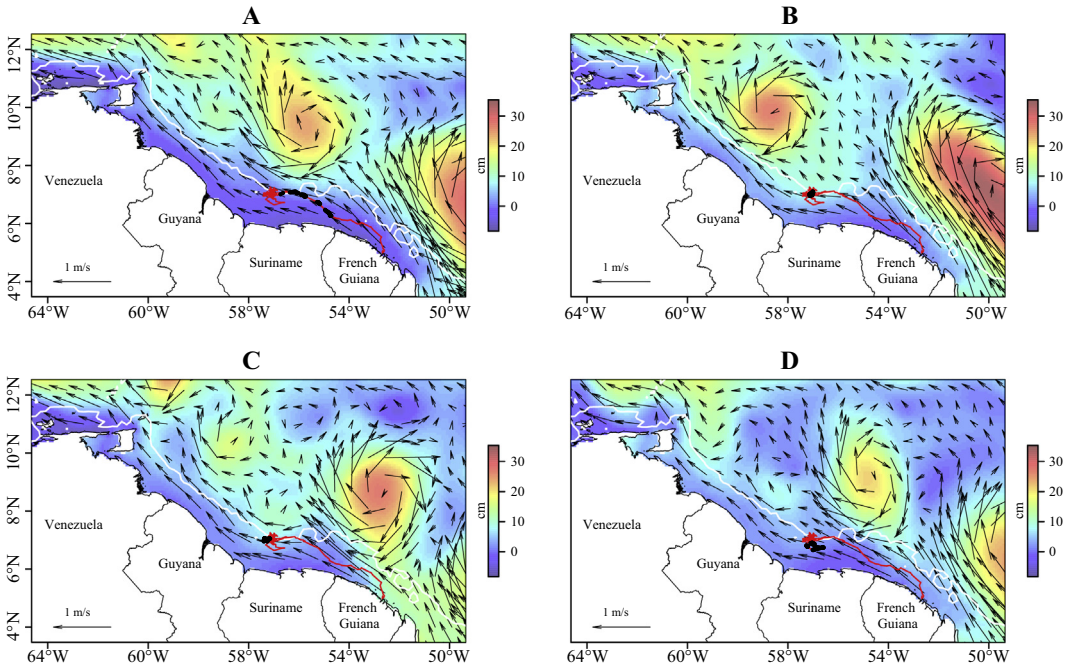

Fig. 2. Averaged direction and velocity of the currents over the whole study area for August 12–18/2013 (A), September 9–15/2013 (B), October 14–20/2013 (C) and November 11–17/2013 (D). The Sea Surface Height (SSH in cm, from the Mercator model) and the trajectory of the turtle #131354 (red solid line) were superimposed on oceanic currents (Mercator model). For a better visual representation, the spatial resolution of the current direction was set to 0.5° decimal. The black dots correspond to the locations of the turtle for the specific day and the white solid line the 100 m isobaths.

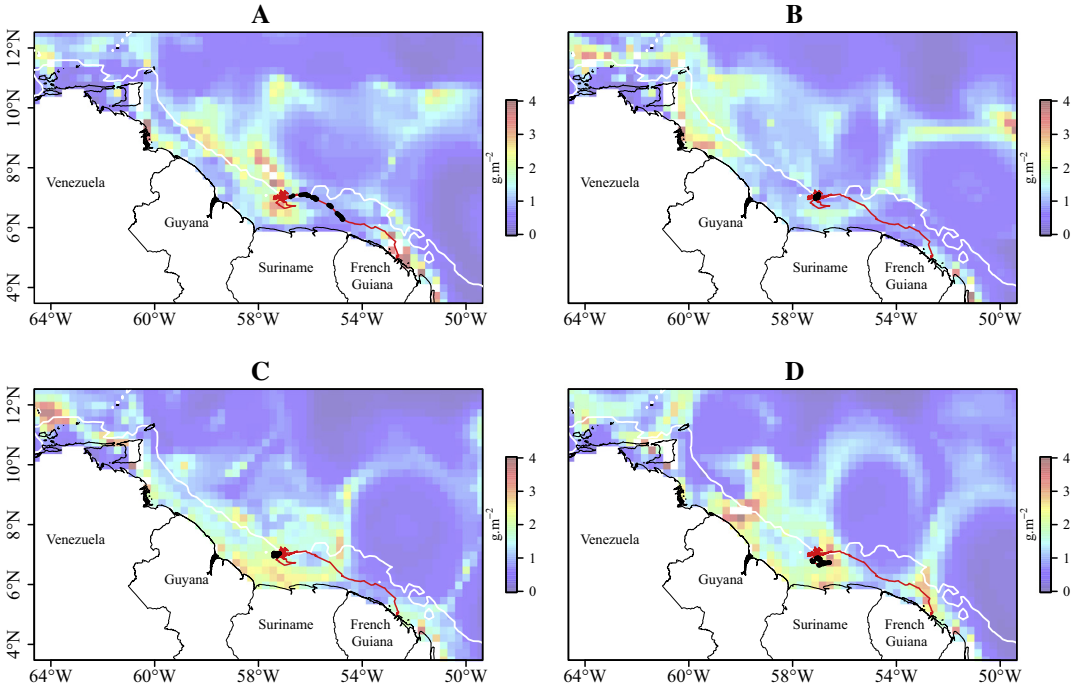

Fig. 3. Averaged micronekton biomass (g WW m^{-2}) predicted from SEAPODYM for August 12–18/2013 (A), September 9–15/2013 (B), October 14–20/2013 (C) and November 11–17/2013 (D) from SEAPODYM. The trajectory of the turtle #131354 (red solid line) was superimposed to micronekton. The black dots correspond to the locations of the turtle for the specific week and the white solid line the 100 m isobaths.

duration. Maximum dive depths varied from 0 to 200 m, with 45% of the dives performed in the upper 50 m (Fig. 4A). Maximum dive depths also differed significantly between individuals (Kruskal–Wallis rank sum test: $p < 0.001$, $n = 4055$).

Dive durations ranged from 30 s to 70 min, with 75% of the dives lasting between 30 and 70 min (Fig. 4B). Maximum dive durations differed significantly between individuals (Kruskal–Wallis rank sum test: $p < 0.001$, $n = 4583$).

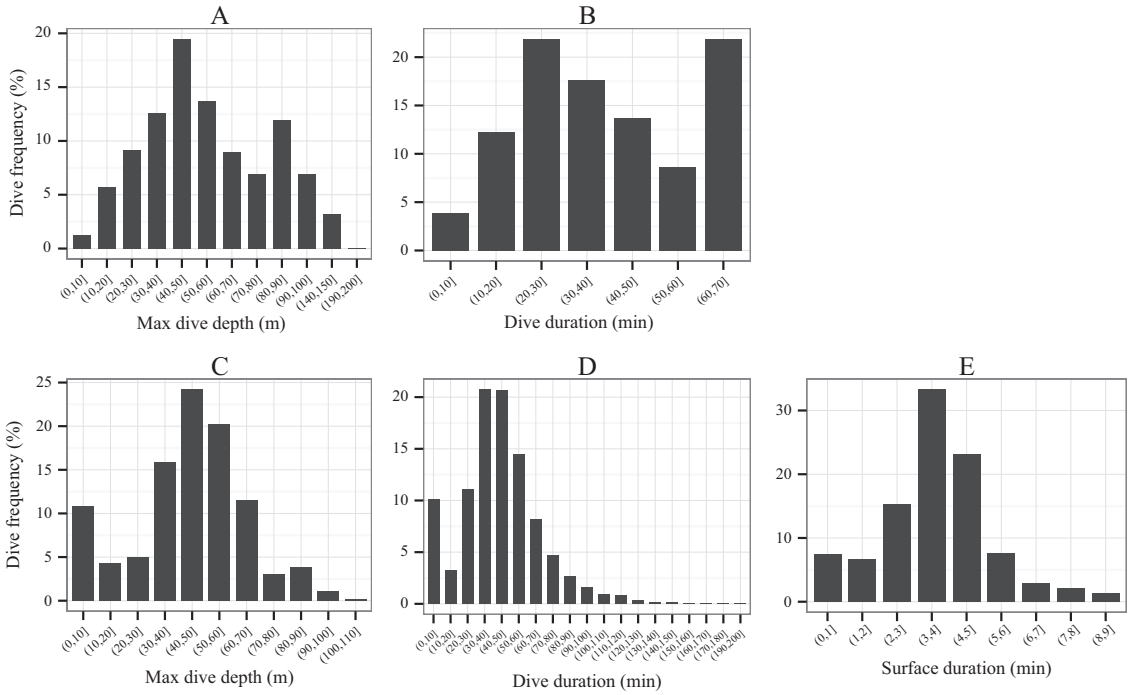

Fig. 4. Histograms of the diving variables recorded by the Argos-linked Fastloc GPS tags (A and B) and the CTD-SRDL tags (C, D and E). Maximum dive depth (A and C, m), dive duration (B and D, min), and post-dive surface interval (E, min) for all individuals.

3.2.2. Diving behavior from CTD-SRDL tags

The CTD-SRDL deployed in 2013 ($n = 2$) and 2014 ($n = 10$) provided reliable data for 2817 summarized dives profiles. Average maximum dive depth was 43.6 ± 20.6 m, ranging from 0 to 110 m (Fig. 4C). Maximum dive depths were significantly different between individuals (Kruskal–Wallis rank sum test, $p < 0.001$, $n = 2817$).

Dive durations varied from 30 s to 200 min (~3 h), lasted on average 45.9 ± 24.5 min and 40% of the dives lasted between 30 and 50 min (Fig. 4D). Dive durations differed significantly between individuals (Kruskal–Wallis rank sum test, $p < 0.001$, $n = 2817$).

Post-dive surface duration ranged from 0.06 s to 8.2 min, for an average duration of 3.6 ± 1.5 min. Sixty percent of the post-dive surface intervals lasted between 3 and 4 min, and differed significantly between individuals (Kruskal–Wallis rank sum test: $p < 0.001$, $n = 2817$) – see Fig. 4E.

Of the 2817 summarized dives retained for the analysis, 44% were benthic dives and 56% were pelagic dives with a difference between bathymetry and maximum dive depth $\geqslant 3$ m. Seventy percent of the turtles performed mainly pelagic dives (#131354, #131355, #130764, #130765, #136773, #136774 and #136779), and three individuals performed exclusively benthic dives (#136772, #136775 and #136778, Fig. 5).

The average Time of Allocation at Depth (TAD) was 0.8 ± 0.1, indicating mainly U-shaped dives (Table 2). Seventy-three percent of the dives recorded by the CTD-SRDL were associated with a TAD ranging between $0.75 \leqslant \text{TAD} < 0.1$.

3.2.3. In situ temperature and salinity data

The 1196 CTD profiles analyzed had recorded 21,775 temperature data and salinity data. Salinity ranged from 7.3 to 36.3 psu, and temperatures from 21.5 to 30.0 °C, and all turtles had used a broad range of oceanographic structures (Fig. 6A). The thermocline depth varied between 26.3 ± 2.3 m and 53.6 ± 9.4 m (#136778 vs. #136773, respectively, Fig. 6B), with an average depth of 43.4 ± 12.3 m (Table 2), and temperature profiles showed a horizontal stratification (Fig. 7A and B).

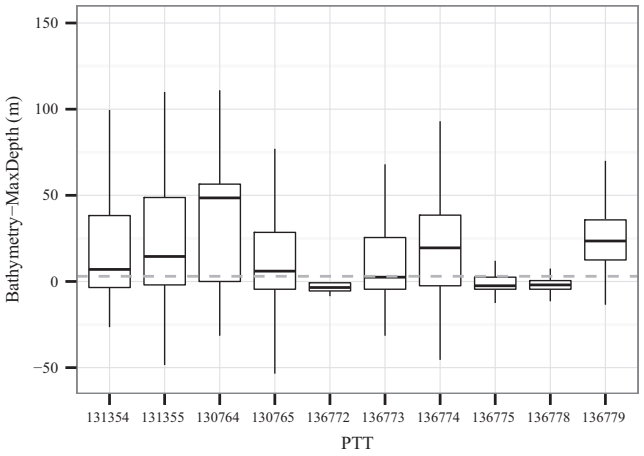

Fig. 5. Box plots of the depth difference between bathymetry and maximum dive depth of the 10 CTD-SRDL tags for each individual. The dotted line refers to the limit between benthic (depth difference $\leqslant 3$ m) and pelagic dives (depth difference >3 m).

3.2.4. Hunting time index

Among the 2817 dives recorded, 77% were discarded due to mismatches between the summarized dive and CTD profiles. Among the 647 remaining dives associated with a CTD profile (only temperature data were used due to the low number of salinity profiles), olive ridleys spent an average 36.4 ± 21.6 min hunting per dive, representing 77 ± 18.3% of the total dive duration (Table 2). Hunting time was negatively related to the euphotic depth and the temperature at mean hunting depth, the latter being the most significant covariate ($p < 0.05$ and $p < 0.001$, respectively, Table 3, Fig. 8A).

3.2.5. Mean hunting depth

The mean hunting depth ranged from 16.0 ± 14.8 to 50.1 ± 14.3 m (#131355 and #131354 respectively), with an

Table 2
Summary of the diving data associated with a temperature profile from CTD-SRDL tags. Values are Mean + SD and numbers in parentheses are the percentages. For each individual, Ndive refers to the number of dives that was associated with a temperature profile.

PTT	Instrument	*N* profile	TAD	Hunting time (min, %)	Hunting depth (m)	Hunting temp (°C)	Thermocline depth (m)
131354	CTD-SRDL	360	0.8 ± 0.1	36.7 ± 17.3 (82)	50.1 ± 14.3	26.0 ± 1.0	50.1 ± 7.3
131355	CTD-SRDL	79	0.8 ± 0.1	15.1 ± 15.0 (68)	16.0 ± 14.8	27.5 ± 0.5	28.8 ± 4.5
130764	CTD-SRDL	23	0.7 ± 0.1	30.4 ± 20.8 (74)	34.2 ± 14.7	26.4 ± 0.9	32.6 ± 4.9
130765	CTD-SRDL	75	0.7 ± 0.1	45.3 ± 36.8 (73)	27.1 ± 19.8	26.0 ± 1.2	36.6 ± 12.5
136772	CTD-SRDL	11	0.6 ± 0.2	27 ± 19.7 (62)	25.6 ± 15.6	26.2 ± 1.1	24.8 ± 4.7
136773	CTD-SRDL	51	0.8 ± 0.1	36.2 ± 25.5 (70)	48.9 ± 31.5	25.2 ± 1.8	53.6 ± 9.4
136774	CTD-SRDL	7	0.8 ± 0.1	39.1 ± 22.2 (68)	35.0 ± 15.7	26.4 ± 0.6	36.9 ± 1.8
136775	CTD-SRDL	16	0.7 ± 0.1	35.9 ± 27.5 (75)	30.3 ± 9.7	27.0 ± 0.6	31.2 ± 6.5
136778	CTD-SRDL	28	0.8 ± 0.1	34.1 ± 13.0 (77)	29.4 ± 6.9	26.7 ± 0.7	26.3 ± 2.3
136779	CTD-SRDL	62	0.7 ± 0.1	31.3 ± 19.2 (71)	35.0 ± 15.4	25.6 ± 1.1	34.2 ± 11.3
		71.2 ± 104.8	0.8 ± 0.1	36.4 ± 21.6 (77 ± 18.3)	43.5 ± 18.5	26.0 ± 1.1	43.4 ± 12.3

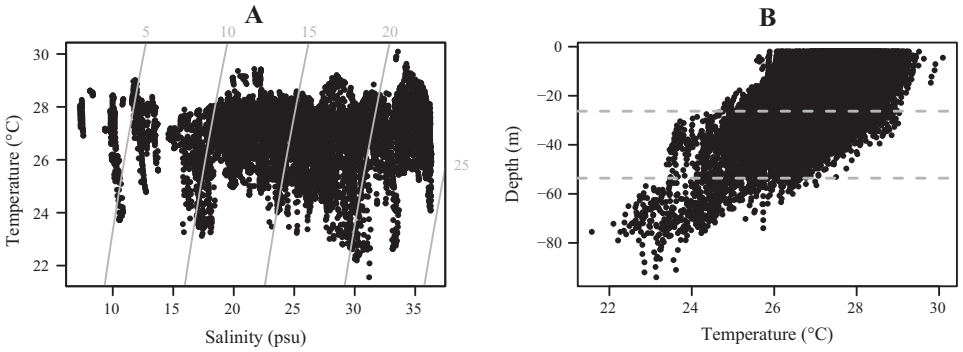

Fig. 6. T–S diagram (A) and temperature profile according to depth (B) for all individuals. The gray lines in A refer to the isopycnal lines and the dotted lines in B to the extrema of the thermocline depth.

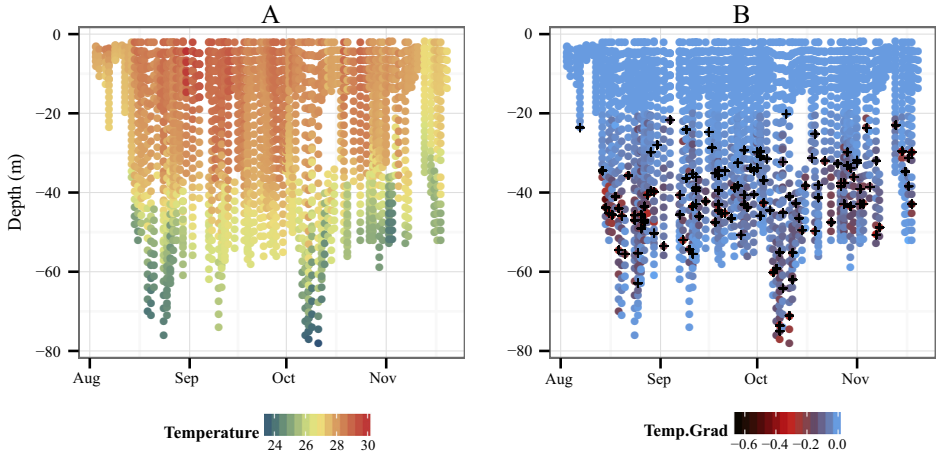

Fig. 7. CTD profiles of the *in situ* temperature (A, in °C) and temperature gradient (B, °C m^{-1}) for the individual #131354 throughout the tracking period. The black crosses in B refer to the mean hunting depths in each profile.

average of 43.5 ± 18.5 m and the average temperature at the mean hunting depth was 26.0 ± 1.1 °C (Table 2). Moreover, mean hunting depth was significantly related to the thermocline depth, the temperature at mean hunting depth and the euphotic depth (Table 4). Mean hunting depth increased with deeper thermocline (Fig. 8B) and euphotic depths ($p < 0.001$ and $p < 0.01$, respectively) and lower temperatures ($p < 0.001$, Table 4, Fig. 8C).

4. Discussion

This is the first study to use satellite telemetry-based movement tracking and diving behavior analysis to identify foraging activity in 18 adult female olive ridley sea turtles in both horizontal and vertical dimensions. We combined remote sensing data (SST, SSH and current velocity), micronekton predictions and *in situ* records (water temperature and salinity) to characterize the foraging activity of *Lepidochelys olivacea* at three different scales:

(1) Across the Guiana basin, taking into account the strong hydrodynamics driven by the retroflection of the North Brazil current.
(2) At the tracking scale, by comparing the habitat used during the transiting and the foraging modes identified.

Table 3
Summary of the selected model designed to relate the hunting time to the oceanographic variables of the water column. "Hunting temp" refers to the temperature at the mean hunting depth.

Response variable	Explanatory variable	Estimate	Std error	*Z* value	*p*-Value
Hunting time ~	Hunting temp	−481.6454	55.08959	−8.742948	<0.001
	Euphotic depth	−179.7802	73.66752	−2.440427	<0.05

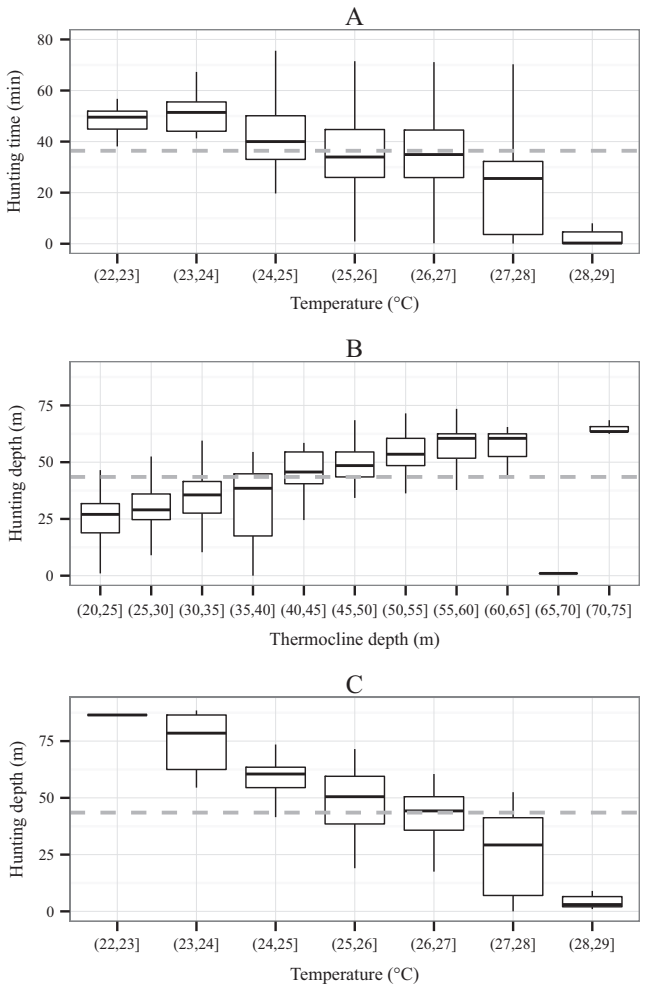

Fig. 8. Box plots of the most significant variables found with the models according to hunting time (A) and hunting depth (B and C). The dotted lines refer to the mean hunting time and mean hunting depth, respectively.

(3) And finally during dives, by relating the foraging activity occurring within dives to the properties of the water column.

4.1. Foraging activity across the Guiana basin

In this study, 18 olive ridleys were satellite tracked over seven months during their post-nesting migration from French Guiana. Although the tracking duration was relatively low for some individuals (mean: 80.7 d, range: 7–229 d), it was similar and even higher than the one of other studies on the same species (Whiting et al., 2007; Swimmer et al., 2009; Plot et al., 2015). Such low tag life could be firstly due to the very low levels of keratin of olive ridleys (Whiting et al., 2007), which prevented from cleaning properly the shell with scrapers to remove the entire epibiotic growth in the attachment area to make the epoxy stick firmly. Another cause of the relatively low tracking duration is probably the high levels of bycatch in the Guiana continental shelf (Fossette et al., 2014), especially regarding olive ridley sea turtles (Chevallier, unpublished data), clearly more subjected to this threat.

All individuals remained exclusively on the continental shelf, which contrasts with data from a previous study (Plot et al., 2015) that describes a higher behavioral plasticity in the migration dispersal, associated with the use of two other domains: continental slope and deep waters. However, all the turtles in our study performed a relatively short migration in terms of duration and distance to the foraging grounds (mean: 366.8 ± 294.5 km and 30 ± 17 d), which is in accordance with other studies on this species (Whiting et al., 2007; Rees et al., 2012; Plot et al., 2015), probably due to the short inter-breeding intervals of one to two years. Olive ridleys are also known to have different patterns in terms of spatial population structure, and the close proximity of the nesting and foraging areas highlighted in the present study is quite of unique.

The Guiana basin is known to be a highly dynamic zone under the influence of both the North Brazil Current and the South Equatorial Counter Current (Pauluhn and Chao, 1999). The merging of these two currents, called the North Brazil retroflection, generates anticyclonic eddies beyond the 500 m isobaths and thus drives the oceanic circulation of the continental shelf (Didden and Schott, 1993; Lumpkin and Garzoli, 2005). By remaining on the neritic domain, olive ridleys seem to target a stable and low turbulent area and therefore avoid being advected by the strong eddies and being swept away by the North Equatorial Counter Current. This occurred for one turtle tracked in 2006, which made a clockwise loop associated with oceanic currents and more specifically with one anticyclonic eddy (Plot et al., 2015). The movements of this single individual, probably due to navigational issues after being advected by the currents, support the idea that olive ridleys may deliberately avoid this highly turbulent area.

The French Guiana continental shelf is a productive zone (Muller-Karger et al., 1988; DeMaster et al., 1996) that is continuously supplied by the Amazon River plume. The warm-core anticyclonic eddies located off the French Guiana continental shelf are characterized by high SSH and SST at their core, and high micronekton biomass at their edge. This could explain why olive ridleys forage in this area during their post-nesting migration. The nutrient supply originating from the Amazon plume aggre-

Table 4
Summary of the selected model designed to relate mean Hunting depth to the oceanographic variables of the water column.

Response variable	Explanatory variable	Estimate	Std error	*Z* value	*p*-Value
Mean hunting depth ~	Thermocline depth	2.81159	0.514215	5.46774	<0.001
	Hunting temp	−12.75975	0.337562	−37.79973	<0.001
	Euphotic depth	1.76262	0.580940	3.03408	<0.01

gates at the edges of these eddies (Froidefond et al., 2002; Baklouti et al., 2007), making the continental shelf an area with a high concentration of organisms, from low- (phytoplankton) to high-trophic levels, including mid-trophic level (micronekton) through bottom-up processes, as shown in the Mozambique Channel (Sabarros et al., 2009). As olive ridley from the Sergipe (northeast Brazil) feeds mainly on crustaceans and small fish (Wildermann and Barrios-Garrido, 2012; Colman et al., 2014), this species is assumed to be a carnivorous consumer at the 3rd of even 4th trophic level. Olive ridleys might therefore target the edges of eddies to access food resources, probably composed of both pelagic and benthic organisms from the different micronekton functional groups, namely crustaceans, cephalopods, fishes and jellyfishes. This is consistent with the generalist feeding behavior of this carnivorous species, which shows a high plasticity (Bjorndal, 1985; McMahon et al., 2007). Stable isotope analyses are planned to be conducted to complete the present study, as skin samples have already been collected, and will be analyzed shortly to shed light on the organisms consumed by olive ridleys during their post-nesting migration along the Guiana coast.

Having described the habitat used by olive ridleys during their migration across the Guiana basin, we then sought to better characterize the habitat of *Lepidochelys olivacea* at their feeding grounds, relating the horizontal foraging activity to oceanographic and biological features provided by ocean circulation models.

4.2. Foraging activity at the tracking scale

Several foraging grounds were identified across the migration route using Residence Time analysis (Barraquand and Benhamou, 2008). The foraging activity occurred in areas of lower current velocity, which suggests that olive ridley sea turtles do indeed target areas of low turbulence rather than being passively advected by eddies. This behavior is supported by the tracking of seven olive ridleys equipped in the same location in 2006 (Plot et al., 2015), which six of them remained on the continental shelf, whereas only one was advected by eddies – see Plot et al., 2015 Supplementary materials. Additionally, turtles migrated in the same direction as the Guiana current, i.e. northwestward, suggesting that they used favorable currents to reach their foraging areas, probably to save energy. Similar patterns were observed in olive ridley turtles during their migration in the North Pacific Ocean, where they moved in the same direction as the North Equatorial Current (Polovina et al., 2006). However, the calculation of the real swimming speed corrected for current velocity indicated that all turtles swam presumably actively throughout the tracking duration. This suggests that they either target favorable habitats, i.e. weak currents, or possibly avoid unfavorable ones characterized by turbulent currents and eddies, as illustrated by the fact that they rapidly leave the strong Guiana current at the beginning of the migration by heading westward, toward less turbulent waters.

To confirm the high swimming speed deduced from the ocean circulation model, it would have been necessary to assess the sensitivity of the Mercator model by using 'control' data from *in situ* surface drifters (Putman and He, 2013; Putman and Mansfield, 2015). However, due to the strong mismatch both in time and space between the satellite-derived outputs and the *in situ* data (http://www.aoml.noaa.gov/phod/dac/dacdata.php), such complementary analysis could not be performed in our study (Fossette et al., 2012a,b). Since we used the Mercator model which provides the highest spatial (0.08°) and temporal (daily) resolutions available to date (comparable to the Global Hybrid Coordinates Ocean Model), Mercator appears to be one of the most sophisticated and reliable tool to simulate ocean dynamics, limiting therefore the differences in velocity between drifter and model outputs ($\sim$3.5 cm s^{-1}) (Putman and He, 2013). As done recently by Putman and Mansfield (2015) on Kemp's ridley and green turtles of the Mexico Gulf, a future study should be dedicated to the deployment of surface drifters alongside olive ridleys from the release site of Remire-Monjoly in French Guiana, to confirm the active swimming behavior of these females during their post-nesting migration.

In addition to the effect of prevailing currents on olive ridleys' displacements, animal-borne instruments are known to induce additional drag, impacting therefore the animal behavior and energetics (Todd Jones et al., 2013). The tracked turtles measured 71.5 ± 2.5 cm (range: 69–75 cm), CCL close to those of Plot et al. (2015) taken on the same population in 2006 (mean: 68.1 ± 1.3 cm). Following Hays' method (2001), CCL were converted into SCL (68.9 ± 2.2 cm) to get an estimate of the drag of each tag type. According to Todd Jones et al. (2013), and given the differences in tag size from both devices used in this study, the estimated drag would increase <5% for a MK10 tag and up to 20% for a CTD-SRDL fixed on a 68.9 cm SCL olive ridley. Furthermore, the swimming speed of the turtles fitted with a CTD-SRDL (0.5 ± 0.03 m s^{-1}) were significantly lower than those fitted with a MK10 tag (0.8 ± 0.18 m s^{-1}, Mann–Whitney U test: $p < 0.001$), this latter being nearly three times lighter than the CTD-SRDL devices (545 g vs. 192 g). Such difference shows the non-negligible effect of different animal-borne instruments on olive ridley's behavior during their energetically costly migration phase. Biotelemetry-induced drag would therefore lead to an underestimation of the real swimming speed of this migratory species, reinforcing the need to deploy surface drifters alongside olive ridleys during their post-nesting migration from French Guiana.

The stable areas targeted are globally associated with high primary productivity, i.e. enriched waters discharged by the Amazon plume, but the foraging activity is not necessarily associated with a specific patch of higher micronekton biomass for all turtles, as the whole continental shelf is characterized by a high productivity. The relatively homogeneous habitats crossed by olive ridleys during their migration could also explain part of this mismatch: differences in terms of environmental values are not always significant when comparing the transiting vs. foraging mode. However, the micronekton biomass remains relatively high in both modes, compared to that found in the core of eddies. Rather than classically considering chlorophyll *a* concentrations or primary production as biological variables (Polovina et al., 2006; Kobayashi et al., 2008; Dalleau et al., 2014), this study is the first to use SEAPODYM outputs to relate olive ridley foraging activity to the distribution of their prey. However, it is important to note that our micronekton data come from model predictions, which are not devoid of uncertainty. In some cases, there can be some differences between the model outputs and *in situ* measurements (Mulet et al., 2012), especially in coastal regions under the influence of a large river such as the Amazon. Given the weekly averaged data of SEAPODYM, the occasional mismatch between olive ridley foraging locations and high micronekton biomass could also be due to the lag between prey distribution and sea turtle movements. However, SEAPODYM outputs are arguably robust enough to provide accurate estimations on the regional scale (Lambert et al., 2014) and provide relative biomass values, which in our case is a sufficient estimation of olive ridley preys. Furthermore, ongoing experiments to validate and assimilate acoustic data are currently being validated to make this model more robust and provide a higher resolution.

As a physiographic variable, deep bathymetry was highly associated with foraging activity as olive ridleys favored deeper waters of between 40 and 200 m at their foraging grounds, probably to avoid the higher water turbidity close to the shore, caused by the nutrient supply from the Amazon and other rivers (Anthony et al., 2010). By targeting clearer waters, turtles could potentially have more visibility to catch prey, while avoiding predators. This

bathymetry is probably also related to diving behavior, characterized by both pelagic and benthic dives.

In accordance with previous studies (McMahon et al., 2007; Hamel et al., 2008; Plot et al., 2015), the dives were mainly U-shaped, i.e. with the core of activity centered at the bottom of the dive (Fedak et al., 2001). Fifty-six percent of the dives were pelagic, and 44% were benthic. Our data confirm that olive ridleys mainly rely on pelagic preys in the Atlantic, and accord with data obtained in the Pacific (Polovina et al., 2006). As previously observed in olive ridleys migrating from French Guiana (Plot et al., 2015), our data also highlight strong differences in the diving behavior among individuals. This could enable this species to use the numerous foraging grounds we identified on the continental shelf, sometimes several hundred kilometers apart. Alternatively, this plasticity could be due the heterogeneity of the local conditions encountered, which probably fluctuate drastically among individuals, and force the turtles to behave differently.

This study enabled us to relate the horizontal foraging activity of olive ridleys to surface environmental variables throughout migration. This species performed a short migration, crossing relatively homogeneous habitats in terms of surface features, namely current velocity, SST, SSH and micronekton biomass. The analysis of the foraging activity in the vertical dimension is complementary and essential, being based on *in situ* data of the water column, and also proved very useful to understand the foraging behavior of olive ridley turtles.

4.3. Foraging activity at the dive scale

By remaining exclusively on the continental shelf, all turtles swam in the tropical surface waters (Stramma and Schott, 1999), but crossed highly stratified waters, especially in terms of salinity. A large number of rivers along the Guianan coast flow into the Equatorial Atlantic, affecting the salinity of the waters (Froidefond et al., 2002) and consequently the primary production and turbidity of the continental shelf. Off the shores of French Guiana, the neritic domain is composed of three water classes that are best distinguished by their reflectance, i.e. beige waters close to the coastline, green waters above the 20 m isobaths and low salinity dark brown waters originating from the Amazon plume (Froidefond et al., 2002). A thick layer of 5–7 m extending up to 80 km offshore is characterized by low salinity, i.e. 17–24 psu, which is consistent with the salinity data recorded by the tags. As turtles focus their foraging activity at depths where salinity variability is thought to be rather limited, it is unlikely that the salinity distribution would act as a major constraint on turtle behavior. Unlike the green waters close to the shore with low chlorophyll *a* concentrations due to high suspended matter, the dark brown waters, i.e. an area off the 20 m isobaths and inhabited by olive ridleys, are characterized by high concentrations of dissolved organic matter and chlorophyll *a*. Our results support the idea that olive ridleys continuously forage during dives in areas of high productivity, with hunting time accounting for an average 77% of the dive duration.

The *in situ* temperatures recorded varied from 21.5 to 30.0 °C, and show a broader thermal range than those seen in previous studies. This is partly because the temperatures recorded in other studies did not have access to *in situ* temperatures and used SST instead (Polovina et al., 2006; McMahon et al., 2007; Swimmer et al., 2009). Comparison of the SST ranges showed that our data (range: 26.1–29.9 °C) are similar to the narrow thermal range of 5 °C observed in olive ridleys studied in the Pacific or those from the Atlantic (Polovina et al., 2006; McMahon et al., 2007; Plot et al., 2015), but with however warmer temperatures. These differences in thermal range may be explained by the warm water supply coming from the Amazon River (Nikiema et al., 2007). As *in situ* temperature plays an important role in the vertical foraging activity of olive ridley sea turtles, hunting time increased with the drop in water temperature. Sea turtles are ectothermic organisms, and may regulate their body temperature by reducing their metabolism thanks to cooler layers within the water column (Caut et al., 2008). The cooler temperatures may also affect the distribution of olive ridley prey.

Thermal stratification in the water column resulted in a thermocline depth ranging from 26.3 to 53.6 m, which is highly correlated to the mean hunting depth. The deeper the thermocline, the hunting depth increased, indicating that olive ridleys preferentially target areas within and below the thermocline depth. Similar behaviors have been reported in seabirds and marine mammals (Ballance et al., 2001; Charrassin and Bost, 2001). The thermocline plays a crucial role in the vertical distribution of pelagic preys (Hakoyama et al., 1994) and ultimately affects the foraging success of marine megafauna species (Benoit-Bird et al., 2013). Also, the sharp change in water temperature induces changes in water density and therefore concentrates organic matter, resulting in a rich source of food for zooplankton. Through bottom-up processes, the micronekton that aggregates at these depths is followed by carnivorous species such as olive ridley sea turtles (Field et al., 2001). By targeting in and below the thermocline depth, *Lepidochelys olivacea* migrating from French Guiana adopt the same behavior as loggerhead turtles from the Pacific, diving at relatively shallow thermocline depths (Polovina et al., 2006). Furthermore, the analysis of stomachal contents performed on olive ridleys caught in Hawaii indicated that this species feeds on pelagic organisms distributed in the subsurface layers of the water column, i.e. pyrosomes (*Pyrosoma atlantica*) and salps (Salpidae) (unpublished data, Honolulu Laboratory, NMFS). The layers of prey aggregation for olive ridleys may therefore be found at and beyond the thermocline depth.

Euphotic depth is the final major oceanographic variable found to play a role on olive ridley foraging activity during dives. Photosynthesis can no longer be supported below this depth due to light deficit (Kirk, 2011), and we observed a longer hunting time in shallower euphotic depths. The prediction of cetacean densities based on SEAPODYM outputs have shown that waters with shallow euphotic depths were associated with higher micronekton biomass in the Southwest Indian Ocean, and conversely, waters with deep euphotic depths in French Polynesia had low micronekton biomass (Lambert et al., 2014). Based on this assumption, the olive ridley may target shallow euphotic depths to access higher concentrations of prey. In contrast, mean hunting depth increased with euphotic depth, suggesting that turtles foraged exclusively within the euphotic zone, where light penetration ensures higher primary production than in deeper layers.

In this study, olive ridley's foraging success was for the first time calculated using the hunting time index as defined in Heerah et al. (2015). Hunting time took up an average 77% of the dive duration, indicating that turtles foraged quasi-continuously during dives, even while transiting (identified via Residence Time Analysis). This result suggests an opportunistic behavior of *Lepidochelys olivacea*, which is consistent with the generalist diet of this species (Bjorndal, 1985; McMahon et al., 2007). However, the lack of high resolution data makes it impossible to validate the vertical speed threshold used to differentiate between transit and hunting modes within-dives. As this approach was adapted from other species, it would be useful to validate this threshold by retrieving the tags during the next inter-nesting season, and thereby also confirm the foraging events detected within each dive. To ensure the correct identification of the different activities of olive ridleys within dives, it would also be interesting to use acceleration data loggers in a further study, as already performed in leatherback turtles (Fossette et al., 2010a,b). This is of particular

interest to glean more information about the diving behavior of olive ridley, which remains little documented to date.

5. Conclusion

The present study describes the foraging behavior of the olive ridley sea turtle in relation to its environment, during post-nesting migration from French Guiana, and significantly reinforces the previous study on the species in this region (Plot et al., 2015). The foraging activity of *Lepidochelys olivacea* was assessed in both horizontal and vertical dimensions through the use of movement tracking data and diving behavior analysis that was carried out via an innovative proxy of the vertical foraging activity, namely the hunting time index. The combination of complementary sources of environmental data and techniques provides a description of the habitat used on three different scales: across the Guiana basin, during the tracking period and within dives. Across the Guiana basin and on the tracking scale, the use of remote sensing data and micronekton predictions highlights the influence of the strong currents that generate anticyclonic eddies and therefore spread the nutrients originating from the Amazon River. This circulation therefore benefits olive ridleys during migration to their feeding grounds. At the finest scale, i.e. the dive level, the use of *in situ* temperature sheds light on the crucial role of the thermocline in the foraging behavior of olive ridleys within dives, suggesting an influence of the temperature in both the regulation of turtle metabolism and prey distribution within the water column. Further investigation into the diet of this species and its foraging activity in the Equatorial Atlantic is required to better understand the feeding ecology of the olive ridley and estimate its prey capture attempts.

Acknowledgements

This study was carried out within the framework of the Plan National d'Action Tortues Marines de Guyane and was produced as part of the CARET2 cooperation project between French Guiana and Suriname, headed by the French Guiana office of WWF-France, in partnership with Kwata NGO, the French National Agency for Hunting and Wildlife (ONCFS), the French Guiana Regional Nature Park (PNRG) and WWF Guianas. The CARET2 program was co-financed by the OP Amazonia with the European Union, the ERDF fund, the Fondation de France, the Ministry of Ecology, Sustainable Development and Energy, and the French National Centre for Space Studies (CNES). It was also supported by the French Guiana Regional Council. PC was supported by Shell and CNES Guyane. The authors also appreciate the support of the ANTIDOT project (Pépinière Interdisciplinaire Guyane, Mission pour l'Interdisciplinarité, CNRS). We would like to thank Anne Corval (CNRS Guyane), Hélène Delvaux (DEAL Guyane) and Eric Hansen (ONCFS DIROM) for their strong support and help in developing this project.

Appendix A. Supplementary material

Supplementary data associated with this article can be found, in the online version, at http://dx.doi.org/10.1016/j.pocean.2016.01.006.

References

Abecassis, M., Senina, I., Lehodey, P., Gaspar, P., Parker, D., Balazs, G., Polovina, J., 2013. A model of loggerhead sea turtle (*Caretta caretta*) habitat and movement in the oceanic North Pacific. PLoS ONE 8, e73274.

Anthony, E.J., Gardel, A., Gratiot, N., Proisy, C., Allison, M.A., Dolique, F., Fromard, F., 2010. The Amazon-influenced muddy coast of South America: a review of mud-bank–shoreline interactions. Earth Science Reviews 103, 99–121.

Bailey, H., Shillinger, G., Palacios, D., Bograd, S., Spotila, J., Paladino, F., Block, B., 2008. Identifying and comparing phases of movement by leatherback turtles using state-space models. Journal of Experimental Marine Biology and Ecology 356, 128–135.

Bailleul, F., Cotté, C., Guinet, C., 2010. Mesoscale eddies as foraging area of a deep-diving predator, the southern elephant seal. Marine Ecology Progress Series 408, 251–264.

Bailleul, F., Pinaud, D., Hindell, M., Charrassin, J., Guinet, C., 2008. Assessment of scale-dependent foraging behaviour in southern elephant seals incorporating the vertical dimension: a development of the First Passage Time method. Journal of Animal Ecology 77, 948–957.

Baklouti, M., Devenon, J.-L., Bourret, A., Froidefond, J.-M., Ternon, J.-F., Fuda, J.-L., 2007. New insights in the French Guiana continental shelf circulation and its relation to the North Brazil Current retroflection. Journal of Geophysical Research: Oceans 112, C02023.

Ballance, L.T., Ainley, D.G., Hunt, J.G., 2001. Seabird foraging ecology. In: Steele, J.H., Thorpe, S.A., Turekian, K.K. (Eds.), Encyclopedia of Ocean Sciences, vol. 5. Academic Press, London, pp. 2636–2644.

Barraquand, F., Benhamou, S., 2008. Animal movements in heterogeneous landscapes: identifying profitable places and homogeneous movement bouts. Ecology 89, 3336–3348.

Baudouin, M., de Thoisy, B., Chambault, P., Berzins, R., Entraygues, M., Kelle, L., Turny, A., Le Maho, Y., Chevallier, D., 2015. Identification of key marine areas for conservation based on satellite tracking of post-nesting migrating green turtles (*Chelonia mydas*). Biological Conservation 184, 36–41.

Benoit-Bird, K.J., Battaile, B.C., Heppell, S.A., Hoover, B., Irons, D., Jones, N., Kuletz, K. J., Nordstrom, C.A., Paredes, R., Suryan, R.M., Waluk, C.M., Trites, A.W., 2013. Prey patch patterns predict habitat use by top marine predators with diverse foraging strategies. PLoS ONE 8, e53348.

Bjorndal, K.A., 1985. Nutritional ecology of sea turtles. Copeia 1985, 736–751.

Boehme, L., Lovell, P., Biuw, M., Roquet, F., Nicholson, J., Thorpe, S., Meredith, M., Fedak, M., 2009. Technical note: animal-borne CTD-satellite relay data loggers for real-time oceanographic data collection. Ocean Science, 685–695.

Brodeur, R.D., Seki, M.P., Pakhomov, E., Suntsov, A.V., 2005. Micronekton-what are they and why are they important. Pacific Marine Science Organization Pices Press 13, 7–11.

Burnham, K.P., Anderson, D.R., Huyvaert, K.P., 2011. AIC model selection and multimodel inference in behavioral ecology: some background, observations, and comparisons. Behavioral Ecology and Sociobiology 65, 23–35.

Calenge, C., 2006. The package "adehabitat" for the R software: a tool for the analysis of space and habitat use by animals. Ecological Modelling 197, 516–519.

Campagna, C., Piola, A.R., Rosa Marin, M., Lewis, M., Fernández, T., 2006. Southern elephant seal trajectories, fronts and eddies in the Brazil/Malvinas confluence. Deep Sea Research Part I: Oceanographic Research Papers 53, 1907–1924.

Caut, S., Guirlet, E., Angulo, E., Das, K., Girondot, M., 2008. Isotope analysis reveals foraging area dichotomy for Atlantic leatherback turtles. PLoS ONE, 4.

Chambault, P., Pinaud, D., Vantrepotte, V., Kelle, L., Entraygues, M., Guinet, C., Berzins, R., Bilo, K., Gaspar, P., De Thoisy, B., Le Maho, Y., Chevallier, D., 2015. Dispersal and diving adjustments of the green turtle *Chelonia mydas* in response to dynamic environmental conditions during post-nesting migration. PLoS ONE 10, e0137340.

Charrassin, J., Bost, C., 2001. Utilisation of the oceanic habitat by king penguins over the annual cycle. Marine Ecology Progress Series 221, 285–297.

Colman, L.P., Sampaio, C.L.S., Weber, M.I., de Castilhos, J.C., 2014. Diet of olive ridley sea turtles, *Lepidochelys olivacea*, in the Waters of Sergipe, Brazil. Chelonian Conservation and Biology 13, 266–271.

Cotté, C., Park, Y.-H., Guinet, C., Bost, C.-A., 2007. Movements of foraging king penguins through marine mesoscale eddies. Proceedings of the Royal Society of London. Series B: Biological Sciences 274, 2385–2391.

Croxall, J.P., 1987. Seabirds: Feeding Ecology and Role in Marine Ecosystems. Cambridge University Press.

Dalleau, M., Benhamou, S., Sudre, J., Ciccione, S., Bourjea, J., 2014. The spatial ecology of juvenile loggerhead turtles (*Caretta caretta*) in the Indian Ocean sheds light on the "lost years" mystery. Marine Biology 161, 1835–1849.

Davis, R.W., Ortega-Ortiz, J.G., Ribic, C.A., Evans, W.E., Biggs, D.C., Ressler, P.H., Cady, R.B., Leben, R.R., Mullin, K.D., Würsig, B., 2002. Cetacean habitat in the northern oceanic Gulf of Mexico. Deep Sea Research Part I: Oceanographic Research Papers 49, 121–142.

DeMaster, D., Smith, W., Nelson, D., Aller, J., 1996. Biogeochemical processes in Amazon shelf waters: chemical distributions and uptake rates of silicon, carbon and nitrogen. Continental Shelf Research 16, 617–643.

Didden, N., Schott, F., 1993. Eddies in the North Brazil Current retroflection region observed by Geosat altimetry. Journal of Geophysical Research: Oceans 98, 20121–20131.

Dragon, A., Bar-Hen, A., Monestiez, P., Guinet, C., 2012. Horizontal and vertical movements as predictors of foraging success in a marine predator. Marine Ecology Progress Series 447, 243–257.

Dragon, A.-C., Monestiez, P., Bar-Hen, A., Guinet, C., 2010. Linking foraging behaviour to physical oceanographic structures: southern elephant seals and mesoscale eddies east of Kerguelen Islands. Progress in Oceanography 87, 61–71.

Fauchald, P., Tveraa, T., 2003. Using first-passage time in the analysis of area-restricted search and habitat selection. Ecology 84, 282–288.

Fauchald, P., Tveraa, T., 2006. Hierarchical patch dynamics and animal movement pattern. Oecologia 149, 383–395.

Fedak, M.A., Lovell, P., Grant, S.M., 2001. Two approaches to compressing and interpreting time-depth information as collected by time-depth recorders and satellite-linked data recorders. Marine Mammal Science 17, 94–110.
Field, I., Hindell, M., Slip, D., Michael, K., 2001. Foraging strategies of southern elephant seals (*Mirounga leonina*) in relation to frontal zones and water masses. Antarctic Science 13, 371–379.
Fossette, S., Georges, J., Tanaka, H., Ropert-Coudert, Y., Ferraroli, S., Arai, N., Sato, K., Naito, Y., Le Maho, Y., 2006. Dispersal and Dive Patterns in Gravid Leatherback Turtles during the Nesting Season in French Guiana. Cornell Univ Libr.
Fossette, S., Gleiss, A., Myers, A.E., Garner, S., Liebsch, N., Whitney, N.M., Hays, G.C., Wilson, R.P., Lutcavage, M.E., 2010a. Behaviour and buoyancy regulation in the deepest-diving reptile: the leatherback turtle. Journal of Experimental Biology 213, 4074–4083.
Fossette, S., Hobson, V.J., Girard, C., Calmettes, B., Gaspar, P., Georges, J.-Y., Hays, G. C., 2010b. Spatio-temporal foraging patterns of a giant zooplanktivore, the leatherback turtle. Journal of Marine Systems 81, 225–234.
Fossette, S., Putman, N.F., Lohmann, K.J., Marsh, R., Hays, G.C., 2012a. A biologist's guide to assessing ocean currents: a review. Marine Ecology Progress Series 457, 285–301.
Fossette, S., Schofield, G., Lilley, M.K.S., Gleiss, A.C., Hays, G.C., 2012b. Acceleration data reveal the energy management strategy of a marine ectotherm during reproduction. Functional Ecology 26, 324–333.
Fossette, S., Witt, M.J., Miller, P., Nalovic, M.A., Albareda, D., Almeida, A.P., Broderick, A.C., Chacón-Chaverri, D., Coyne, M.S., Domingo, A., Eckert, S., Evans, D., Fallabrino, A., Ferraroli, S., Formia, A., Giffoni, B., Hays, G.C., Hughes, G., Kelle, L., Leslie, A., López-Mendilaharsu, M., Luschi, P., Prosdocimi, L., Rodriguez-Heredia, S., Turny, A., Verhage, S., Godley, B.J., 2014. Pan-Atlantic analysis of the overlap of a highly migratory species, the leatherback turtle, with pelagic longline fisheries. Proceedings of the Royal Society of London. Series B: Biological Sciences 281, 20133065.
Fratantoni, D.M., Richardson, P.L., 2006. The evolution and demise of North Brazil current rings. Journal of Physical Oceanography 36, 1241–1264.
Froidefond, J.-M., Gardel, L., Guiral, D., Parra, M., Ternon, J.-F., 2002. Spectral remote sensing reflectances of coastal waters in French Guiana under the Amazon influence. Remote Sensing of Environment 80, 225–232.
Fuiman, L., Davis, R., Williams, T., 2002. Behavior of midwater fishes under the Antarctic ice: observations by a predator. Marine Biology 140, 815–822.
Gaspar, P., Georges, J.-Y., Fossette, S., Lenoble, A., Ferraroli, S., Maho, Y.L., 2006. Marine animal behaviour: neglecting ocean currents can lead us up the wrong track. Proceedings of the Royal Society of London B: Biological Sciences 273, 2697–2702.
Georges, J.Y., Billes, A., Ferraroli, S., Fossette, S., Fretey, J., Grémillet, D., Maho, Y.L., Myers, A.E., Tanaka, H., Hays, G.C., 2007. Meta-analysis of movements in Atlantic leatherback turtles during nesting season: conservation implications. Quantitative Biology: Populations and Evolution, arXiv:q-bio/0701040.
Grinnell, J., 1917. Field tests of theories concerning distributional control. American Naturalist 51, 115–128.
Hakoyama, H., Boeuf, B.J.L., Naito, Y., Sakamoto, W., 1994. Diving behavior in relation to ambient water temperature in northern elephant seals. Canadian Journal of Zoology 72, 643–651.
Hamel, M.A., McMahon, C.R., Bradshaw, C.J.A., 2008. Flexible inter-nesting behaviour of generalist olive ridley turtles in Australia. Journal of Experimental Marine Biology and Ecology 359, 47–54.
Hays, G.C., 2001. The implications of adult morphology for clutch size in the flatback turtle (*Natator depressa*). Journal of the Marine Biological Association of the UK 81, 1063–1064.
Heerah, K., Hindell, M., Guinet, C., Charrassin, J.-B., 2014. A new method to quantify within dive foraging behaviour in marine predators. PLoS ONE 9, e99329.
Heerah, K., Hindell, M., Guinet, C., Charrassin, J.-B., 2015. From high-resolution to low-resolution dive datasets: a new index to quantify the foraging effort of marine predators. Animal Biotelemetry 3, 1–12.
Houston, A.I., Carbone, C., 1992. The optimal allocation of time during the diving cycle. Behavioral Ecology 3, 255–265.
Jonsen, I.D., Flemming, J.M., Myers, R.A., 2005. Robust state–space modeling of animal movement data. Ecology 86, 2874–2880.
Jonsen, I.D., Myers, R.A., James, M.C., 2006. Robust hierarchical state–space models reveal diel variation in travel rates of migrating leatherback turtles. Journal of Animal Ecology 75, 1046–1057.
Jonsen, I., Myers, R.A., James, C., 2007. Identifying leatherback turtle foraging behaviour from satellite telemetry using a switching state-space model. Marine Ecology Progress Series 337, 255–264.
Kareiva, P., Odell, G., 1987. Swarms of predators exhibit "preytaxis" if individual predators use area-restricted search. American Naturalist 130, 233–270.
Kelle, L., Gratiot, N., De Thoisy, B., 2009. Olive ridley turtle *Lepidochelys olivacea* in French Guiana: back from the brink of regional extirpation? Oryx 43, 243–246.
Kirk, J.T., 2011. Light and Photosynthesis in Aquatic Ecosystems Camb Univ Press.
Kobayashi, D.R., Polovina, J.J., Parker, D.M., Kamezaki, N., Cheng, I.-J., Uchida, I., Dutton, P.H., Balazs, G.H., 2008. Pelagic habitat characterization of loggerhead sea turtles, *Caretta caretta*, in the North Pacific Ocean (1997–2006): insights from satellite tag tracking and remotely sensed data. Journal of Experimental Marine Biology and Ecology 356, 96–114.
Labrousse, S., Vacquié-Garcia, J., Heerah, K., Guinet, C., Sallee, J.-B., Authier, M., Picard, B., Roquet, F., Bailleul, F., Hindell, M., Charrassin, J.-B., 2015. Winter use of sea ice and ocean water-mass habitat by southern elephant seals: the length and breadth of the mystery. Progress in Oceanography.
Lambardi, P., Lutjeharms, J.R.E., Mencacci, R., Hays, G.C., Luschi, P., 2008. Influence of ocean currents on long-distance movement of leatherback sea turtles in the Southwest Indian Ocean. Marine Ecology Progress Series 353, 289–301.
Lambert, C., Mannocci, L., Lehodey, P., Ridoux, V., 2014. Predicting cetacean habitats from their energetic needs and the distribution of their prey in two contrasted tropical regions. PLoS ONE 9, e105958.
Lavielle, M., 2005. Using penalized contrasts for the change-point problem. Signal Processing 85, 1501–1510.
Lehodey, P., Murtugudde, R., Senina, I., 2010a. Bridging the gap from ocean models to population dynamics of large marine predators: a model of mid-trophic functional groups. Progress in Oceanography 84, 69–84.
Lehodey, P., Senina, I., Calmettes, B., Hampton, J., Nicol, S., 2012. Modelling the impact of climate change on Pacific skipjack tuna population and fisheries. Climate Change 119, 95–109.
Lehodey, P., Senina, I., Murtugudde, R., 2008. A spatial ecosystem and populations dynamics model (SEAPODYM) – modeling of tuna and tuna-like populations. Progress in Oceanography 78, 304–318.
Lehodey, P., Senina, I., Sibert, J., Bopp, L., Calmettes, B., Hampton, J., Murtugudde, R., 2010b. Preliminary forecasts of Pacific bigeye tuna population trends under the A2 IPCC scenario. Progress in Oceanography 86, 302–315.
Lévy, M., 2008. The modulation of biological production by oceanic mesoscale turbulence. In: Weiss, J.B., Provenzale, A. (Eds.), Transport and Mixing in Geophysical Flows. Springer, Berlin Heidelberg, pp. 219–261.
Lopez, R., Malarde, J.-P., Royer, F., Gaspar, P., 2014. Improving Argos Doppler location using multiple-model Kalman filtering. IEEE Transactions on Geoscience and Remote Sensing 52, 4744–4755.
Lumpkin, R., Garzoli, S.L., 2005. Near-surface circulation in the Tropical Atlantic Ocean. Deep Sea Research Part I: Oceanographic Research Papers 52, 495–518.
Luque, S., 2007. Diving behaviour analysis in R. R News 7, 8–14.
McMahon, C., Bradshaw, C., Hays, G., 2007. Satellite tracking reveals unusual diving characteristics for a marine reptile, the olive ridley turtle *Lepidochelys olivacea*. Marine Ecology Progress Series 329, 239–252.
Meade, R.H., 1996. River-sediment inputs to major deltas. In: Sea-Level Rise and Coastal Subsidence: Causes, Consequences, and Strategies. Kluwer Acad, Norvwell, pp. 63–85.
Mitani, Y., Sato, K., Ito, S., Cameron, M.F., Siniff, D.B., Naito, Y., 2003. A method for reconstructing three-dimensional dive profiles of marine mammals using geomagnetic intensity data: results from two lactating Weddell seals. Polar Biology 26, 311–317.
Mulet, S., Rio, M.-H., Mignot, A., Guinehut, S., Morrow, R., 2012. A new estimate of the global 3D geostrophic ocean circulation based on satellite data and in-situ measurements. Deep Sea Research Part II: Topical Studies in Oceanography 77–80, 70–81.
Muller-Karger, F.E., McClain, C.R., Richardson, P.L., 1988. The dispersal of the Amazon's water. Nature 333, 56–59.
Nikiema, O., Devenon, J.-L., Baklouti, M., 2007. Numerical modeling of the Amazon River plume. Continental Shelf Research 27, 873–899.
Okuyama, J., Kawabata, Y., Naito, Y., Arai, N., Kobayashi, M., 2009. Monitoring beak movements with an acceleration datalogger: a useful technique for assessing the feeding and breathing behaviors of sea turtles. Endanger Species Research 10, 39–45.
Pauluhn, A., Chao, Y., 1999. Tracking eddies in the subtropical North-Western Atlantic Ocean. Physics and Chemistry of the Earth, Part A: Solid Earth and Geodesy 24, 415–421.
Péron, C., Delord, K., Philipps, A., Charbonnier, Y., Marteau, C., Louzao, M., Weimerskirch, H., 2010. Seasonal variation in oceanographic habitat and behaviour of white-chinned petrels *Procellaria aequinoctialis* from Kerguelen Island. Marine Ecology Progress Series 416, 267–284.
Pinaud, D., 2008. Quantifying search effort of moving animals at several spatial scales using first-passage time analysis: effect of the structure of environment and tracking systems. Journal of Applied Ecology 45, 91–99.
Pinaud, D., Weimerskirch, H., 2005. Scale-dependent habitat use in a long-ranging central place predator. Journal of Animal Ecology 74, 852–863.
Pinheiro, J., Bates, D., DebRoy, S., Sarkar, D., R Core Team, 2015. nlme: Linear and Nonlinear Mixed Effects Models. R Package Version 3.1-120.
Plot, V., De Thoisy, B., Georges, J., 2015. Dispersal and dive patterns during the post-nesting migration of olive ridley turtles from French Guiana. Endanger Species Research 26, 221–234.
Polovina, J.J., Balazs, G.H., Howell, E.A., Parker, D.M., Seki, M.P., Dutton, P.H., 2004. Forage and migration habitat of loggerhead (*Caretta caretta*) and olive ridley (*Lepidochelys olivacea*) sea turtles in the central North Pacific Ocean. Fisheries Oceanography 13, 36–51.
Polovina, J., Uchida, I., Balazs, G., Howell, E.A., Parker, D., Dutton, P., 2006. The Kuroshio extension bifurcation region: a pelagic hotspot for juvenile loggerhead sea turtles. Deep Sea Research Part II: Topical Studies in Oceanography 53, 326–339.
Putman, N.F., He, R., 2013. Tracking the long-distance dispersal of marine organisms: sensitivity to ocean model resolution. Journal of the Royal Society Interface 10, 20120979.
Putman, N.F., Mansfield, K.L., 2015. Direct evidence of swimming demonstrates active dispersal in the sea turtle "Lost Years". Current Biology 25, 1221–1227.
R Core Team, 2014. R: A Language and Environment for Statistical Computing. R Foundation for Statistical Computing, Vienna, Austria. <http://www.R-project.org/>.
Rees, A., Al-Kiyumi, A., Broderick, A., Papathanasopoulou, N., Godley, B., 2012. Conservation related insights into the behaviour of the olive ridley sea turtle

Lepidochelys olivacea nesting in Oman. Marine Ecology Progress Series 450, 195–205.

Robinson, P.W., Tremblay, Y., Crocker, D.E., Kappes, M.A., Kuhn, C.E., Shaffer, S.A., Simmons, S.E., Costa, D.P., 2007. A comparison of indirect measures of feeding behaviour based on ARGOS tracking data. Deep Sea Research Part II: Topical Studies in Oceanography 54, 356–368.

Roquet, F., Charrassin, J.-B., Marchand, S., Boehme, L., Fedak, M., Reverdin, G., Guinet, C., 2011. Delayed-mode calibration of hydrographic data obtained from animal-borne satellite relay data loggers. Journal of Atmospheric and Oceanic Technology 28, 787–801.

Roquet, F., Wunsch, C., Forget, G., Heimbach, P., Guinet, C., Reverdin, G., Charrassin, J.-B., Bailleul, F., Costa, D.P., Huckstadt, L.A., Goetz, K.T., Kovacs, K.M., Lydersen, C., Biuw, M., Nøst, O.A., Bornemann, H., Ploetz, J., Bester, M.N., McIntyre, T., Muelbert, M.C., Hindell, M.A., McMahon, C.R., Williams, G., Harcourt, R., Field, I. C., Chafik, L., Nicholls, K.W., Boehme, L., Fedak, M.A., 2013. Estimates of the Southern Ocean general circulation improved by animal-borne instruments. Geophysical Research Letters 40, 2013GL058304.

Sabarros, P.S., Ménard, F., Lévénez, J.-J., Tew-Kai, E., Ternon, J.-F., 2009. Mesoscale eddies influence distribution and aggregation patterns of micronekton in the Mozambique Channel. Marine Ecology Progress Series 395, 101–109.

Sibert, J., Senina, I., Lehodey, P., Hampton, J., 2012. Shifting from marine reserves to maritime zoning for conservation of Pacific bigeye tuna (*Thunnus obesus*). Proceedings of the National Academy of Sciences 109, 18221–18225.

Silva, M.A., Jonsen, I., Russel, D.J., Prieto, R., Thompson, D., 2014. Assessing performance of bayesian state-space models fit to Argos satellite telemetry locations processed with Kalman filtering. PLoS ONE, 9.

Stammer, D., Wunsch, C., 1999. Temporal changes in eddy energy of the oceans. Deep Sea Research Part II: Topical Studies in Oceanography 46, 77–108.

Stramma, L., Schott, F., 1999. The mean flow field of the tropical Atlantic Ocean. Deep Sea Research Part II: Topical Studies in Oceanography 46, 279–303.

Swimmer, Y., McNaughton, L., Foley, D., Moxey, L., Nielsen, A., 2009. Movements of olive ridley sea turtles *Lepidochelys olivacea* and associated oceanographic features as determined by improved light-based geolocation. Endanger Species Research 10, 245–254.

Tew-Kai, E., Marsac, F., 2009. Patterns of variability of sea surface chlorophyll in the Mozambique Channel: a quantitative approach. Journal of Marine Systems 77, 77–88.

Todd Jones, T., Van Houtan, K.S., Bostrom, B.L., Ostafichuk, P., Mikkelsen, J., Tezcan, E., Carey, M., Imlach, B., Seminoff, J.A., 2013. Calculating the ecological impacts of animal-borne instruments on aquatic organisms. Methods in Ecology and Evolution 4, 1178–1186.

VanDerWal, J., Falconi, L., Januchowski, S., Shoo, L., Storlie, C., 2014. SDMTools: Species Distribution Modelling Tools: Tools for Processing Data associated with Species Distribution Modelling Exercises. R Package Version 1.1–221.

Viviant, M., Monestiez, P., Guinet, C., 2014. Can we predict foraging success in a marine predator from dive patterns only? Validation with prey capture attempt data. PLoS ONE 9, e88503.

Watanabe, Y., Mitani, Y., Sato, K., Cameron, M.F., Naito, Y., 2003. Dive depths of Weddell seals in relation to vertical prey distribution as estimated by image data. Marine Ecology Progress Series 252, 283–288.

Weimerskirch, H., Le Corre, M., Jaquemet, S., Potier, M., Marsac, F., 2004. Foraging strategy of a top predator in tropical waters: great frigatebirds in the Mozambique Channel. Marine Ecology Progress Series 275, 297–308.

Whiting, S., Long, J., Coyne, M., 2007. Migration routes and foraging behaviour of olive ridley turtles *Lepidochelys olivacea* in northern Australia. Endanger Species Research 3, 1–9.

Wildermann, N.E., Barrios-Garrido, H., 2012. First report of Callinectes sapidus (Decapoda: Portunidae) in the diet of *Lepidochelys olivacea*. Chelonian Conservation and Biology 11, 265–268.

Zuur, A., Ieno, E.N., Walker, N., Saveliev, A.A., Smith, G.M., 2009. Mixed Effects Models and Extensions in Ecology with R. Springer Science & Business Media.